Applied Catalysis B: Environmental 166–167 (2015) 313–319

Contents lists available at ScienceDirect

Applied Catalysis B: Environmental

journal homepage: www.elsevier.com/locate/apcatb

Role of CeO_2 as oxygen promoter in the accelerated photocatalytic degradation of phenol over rutile TiO_2

Zhen Li, Jiayi Sheng, Yuhong Zhang, Xiaojin Li, Yiming Xu*

State Key Laboratory of Silicon Materials and Department of Chemistry, Zhejiang University, Hangzhou 310027, PR China

ARTICLE INFO

Article history:
Received 11 September 2014
Received in revised form 6 November 2014
Accepted 15 November 2014
Available online 22 November 2014

Keywords:
Titanium oxide
Cerium oxide
Photocatalysis
Organic degradation
Oxygen defects

ABSTRACT

In this work, we report that the nonstoichiometric CeO_2 prepared at low temperature has ability to store and release oxygen to rutile TiO_2, improving phenol degradation in aerated aqueous suspension under UV light. The biphase oxide was prepared by mixing individual oxides together, without obvious changes of TiO_2 phase, in terms of the crystallite size, surface area and band gap energy. As the amount of CeO_2 in CeO_2/TiO_2 increased, the photocatalytic activity of the mixed oxide increased, and then decreased. The optimal CeO_2 loading was about 1.5 wt%, which increased the activity of TiO_2 by 60%. Strikingly, as the synthesis temperature for CeO_2 and TiO_2 increased, the activity enhancement of TiO_2 decreased and increased, respectively. Moreover, CeO_2 was also positive to the production of H_2O_2 over the irradiated rutile TiO_2. However, a similar loading of CeO_2 onto anatase and P25 TiO_2 led to slight decrease in the photocatalytic activity for phenol degradation. By using silver ions as electron scavengers, none of the above TiO_2 samples showed an activity enhancement on the addition of CeO_2. Although these oxides have different conduction band edge potentials, the possible charge transfer between TiO_2 and CeO_2 is excluded. A plausible mechanism responsible for the observed activity difference among the samples is proposed.

1. Introduction

Photocatalytic degradation of organic pollutants on TiO_2 as a potential new technology for air purification and water treatment has been studied for more than 30 years [1–3]. It is now widely recognized that over the UV light excited TiO_2, a variety of organic pollutants can degrade into CO_2, and small fragments at ambient temperature and pressure only using O_2 as oxidant. However, the efficiency of TiO_2 photocatalysis for organic degradation achieved so far is still not high enough to enable practical application [4]. This is because the photogenerated conduction band electrons (e_{cb}^-) and valence band holes (h_{vb}^+) of TiO_2 easily recombine to heat, without net chemical reactions with surface sorbates. To improve the efficiency of charge separation, and then to increase the quantum yield of organic degradation, one of the strategies is not only to increase the crystallinity of TiO_2 [5–7], but also to enrich the dissolved O_2 onto the oxide surface from aqueous solution [8,9].

It is well known that ceria is a good oxygen promoter for the catalytic removal of CO, NO_x and hydrocarbons in the automotive exhaust [10–13]. There are many oxygen vacancies and Ce^{3+} defects present in CeO_{2-x}. Under lean fuel conditions, CeO_{2-x} adsorbs oxygen in the forms of $O_2^{\bullet-}$ and O_2^{2-}. Under rich fuel conditions, the stored oxygen in CeO_2 is released with regeneration of CeO_{2-x}. With respect to TiO_2 photocatalysis, O_2 is definitely required, because it is not only an oxidant of organic pollutants, but also acts as an electron scavenger of the irradiated TiO_2 to prevent the electron-hole recombination. Then, ceria might be also a good oxygen promoter of TiO_2 photocatalysis for organic degradation at the solid–liquid interface, which has not been reported yet in the literature.

On the other hand, CeO_2 is a n-type semiconductor, and has been recently used as a photocatalyst for organic dye degradation in water [14,15]. Since TiO_2 and CeO_2 have different band structures, their coupling may result into the improved photocatalytic activity for organic degradation. In fact, many papers have claimed that a CeO_2-modified TiO_2 (denoted as CeO_2/TiO_2) is more active than TiO_2 for organic degradation either under UV [16–23] or visible light [24–27]. The observed activity of CeO_2/TiO_2 higher than that of TiO_2 is presumably ascribed to the electron transfer from the irradiated TiO_2 to CeO_2, consequently improving the efficiency of charge separation and accelerating organic degradation. However, in these studies, CeO_2/TiO_2 and TiO_2 were prepared from the hydrolysis of Ti(IV) precursor in the presence and absence of Ce(III) salt, respectively, followed by thermal treatment. As a result, the physical properties of TiO_2 in CeO_2/TiO_2 were notably different

* Corresponding author. Tel.: +86 571 87952410; fax: +86 571 87951895.
E-mail address: xuym@zju.edu.cn (Y. Xu).

http://dx.doi.org/10.1016/j.apcatb.2014.11.029
0926-3373/

from those of bare TiO_2, including the crystallite size and phase composition [15–26]. It is known that the *apparent* photocatalytic activity of TiO_2 greatly changes with its physical parameters [1–3]. Then, the observed higher activity of CeO_2/TiO_2 than that of TiO_2 may be simply due to the changes of TiO_2 phase [28], not due to the interfacial charge transfer between CeO_2 and TiO_2. In other words, the role of CeO_2 in the enhanced photocatalytic activity of CeO_2/TiO_2 still remains incompletely elucidated. To make clear the effect of CeO_2, the TiO_2 phase in different CeO_2/TiO_2 samples should be controlled the same as much as possible. Furthermore, nearly all of these studies about the CeO_2 effect have been made with anatase TiO_2, but a little has been done with rutile TiO_2 [23], probably due to the poor photoactivity of rutile as compared to anatase. In a previous study, we have shown that the *intrinsic* photocatalytic activity of TiO_2 exponentially increases with its sintering temperature, regardless of the solid structures in the forms of anatase, rutile and their mixture [7,29,30]. Anatase TiO_2 that has a higher *apparent* photocatalytic activity than that of rutile is ascribed to its higher uptake of O_2 from an aerated aqueous solution. Rutile TiO_2 is the most stable than anatase, and it can be prepared at a high temperature without problem of phase transition [2]. To develop a highly active and stable photocatalyst, the CeO_2-modified rutile is worthy of being further investigated.

In this study, the effect of CeO_2 loading on the photocatalytic activity of rutile TiO_2 has been examined in details. The biphase oxide was prepared by a simple mixing of individual oxides in isopropanol, followed by dryness at 90 °C. Prior to use, both CeO_2 and TiO_2 were home-made at a temperature higher than 90 °C, so that the TiO_2 phase in CeO_2/TiO_2 would remain the same as that of parent TiO_2. The solid was characterized with X-ray diffraction, N_2 adsorption, and UV–vis diffuse reflectance spectroscopy, while the solid photoactivity was evaluated using phenol degradation as a model reaction. Photoreaction was conducted in an aqueous solution under UV light at wavelengths equal and longer than 320 nm. Under these conditions, phenol photolysis and its dark adsorption on the metal oxide were both negligible. This would simplify the activity measurement, without the need to examine the effect of organic photolysis, adsorption and dye sensitization on the rate of organic degradation. Several influencing factors were examined, including the CeO_2 loading, and the synthesis temperature of bare oxide, and the crystal structure of TiO_2. Furthermore, the production of H_2O_2, and the conduction band edge potentials for the oxides were also measured.

2. Experimental

2.1. Materials

Ceria was prepared from the thermal decomposition of cerium (III) acetate (Sigma–Aldrich) in air at 400–900 °C for 3 h. Thermal analysis confirmed that cerium precursor completely decomposed to CeO_2 at 300 °C (Fig. S1, Supplementary data). Rutile TiO_2 (denoted as sRT) was prepared by the hydrolysis of $TiCl_4$ (Shanghai Chemicals, Inc.) in an iced bath, followed by heating at 60 °C for 2 h [31]. After the suspension cooled down to room temperature, the white precipitates were filtrated, and thoroughly washed with a Milli-Q ultrapure water, until no Cl^- ions were detectable by $AgNO_3$ in the filtrate. Finally, the white solid was dried at 60 °C in a vacuum oven, and then sintered in air at 200–900 °C for 3 h. Moreover, for a comparison, anatase TiO_2 (cAT), and P25 TiO_2 (P25), obtained from Sigma–Aldrich, and Degussa Corporation, respectively, were also examined in this study.

The above oxides were then used for the preparation of CeO_2/TiO_2. Typically, TiO_2 was mixed with 1.5 wt% of CeO_2 in 50 mL of isopropanol, followed by sonification and magnetic stirring for 1.5 h. After that, the suspension was dried slowly at 90 °C in a fume hood. Finally, the solid was ground, and used thereafter as photocatalysts. Considering that this treatment may change the physical properties of the oxide, each bare TiO_2 (CeO_2) in the absence of CeO_2 (TiO_2) was also treated by following the above procedure, and used thereafter as a reference photocatalyst.

2.2. Characterization

X-ray diffraction (XRD) pattern was recorded on a D/max-2550/PC diffractometer (Rigaku) with a Cu $K\alpha$ as the irradiation source, operated at 40 kV and 40 mA. The crystal diameters (d_{XRD}) of the oxides were calculated by using Scherrer equation, based on the integrated intensities of (1 1 0) rutile, (1 0 1) anatase and (1 1 1) CeO_2. Adsorption–desorption isotherms of N_2 on solid were measured at 77 K on a Micromeritics ASAP2020 apparatus. From the adsorption and desorption branches of the isotherm, the Brunauer–Emmett–Teller (BET) specific surface area (A_{sp}) and total pore volume (V_p) were calculated, respectively. Diffuse reflectance spectra (DRS) were recorded on a Shimadzu UV-2550 using $BaSO_4$ as a reference. The measured reflectance (R) was transferred into the Kubelka–Munk (K–M) absorbance, $F_R = (1-R)^2/(2R)$. The band gap energies (E_g) for TiO_2 and CeO_2 were estimated by following the literature procedure [32].

2.3. Photocatalysis and analysis

Experiments were carried out at 25 °C in a Pyrex-glass reactor. Unless stated otherwise, the initial concentrations of catalyst, phenol, and $AgNO_3$ were set at 1.0 g/L, 0.43 mM, and 1.0 mM, respectively. The reaction suspension was first stirred in the dark for 2 h, and then irradiated through a Pyrex-glass filter with a high pressure mercury lamp (375 W, Shanghai Mengya, China). At given intervals, 3.0 mL of the suspension was withdrawn, filtered through a membrane, and immediately analyzed by HPLC (high performance liquid chromatography) on a Dionex P680 (Apollo C18 reverse column, and 50% CH_3OH aqueous solution as an eluent). When the reaction was conducted in the presence $AgNO_3$, the suspension was purged with N_2 (99.99%) for 0.5 h, and then sealed off for experiments. Silver ion was measured on an Agilent 8451 spectrometer at 472 nm through its complex with p-dimethylaminobenzalrhodanine [33]. Hydrogen peroxide was quantified at 551 nm through its reaction with N,N-diethyl-1,4-phenolenediammonium catalyzed by peroxidase [34].

3. Results and discussion

3.1. Solid characterization

In this study, more than 20 samples were prepared, and characterized with XRD, N_2 adsorption and DRS. These results are summarized in Supplementary data. In brief, the XRD patterns of bare CeO_2, sRT and cAT (Fig. 1) were in good agreement with those of cubic fluorite (PDF no. 34-0394), rutile (PDF no. 21-1276), and anatase (PDF no. 21-1272), respectively, whereas P25 showed a mixed XRD pattern of 20% rutile and 80% anatase. After TiO_2 was mixed with 1.5 wt% of CeO_2, the XRD pattern of TiO_2 remained nearly unchanged in its peak intensity, crystallite size, and cell parameters. The diffractions of cubic CeO_2 were not detectable until its amount in CeO_2/TiO_2 was higher than 5 wt%. However, the BET surface area and total pore volume of CeO_2/TiO_2, measured by N_2 adsorption at 77 K, were somewhat lower or higher than those calculated from bare CeO_2 and TiO_2. Since N_2 largely adsorbs onto the external surfaces of aggregates, it follows that there are some interaction between CeO_2 and sRT, which alters the degree of particle aggregation, and porous networks as well. Furthermore, the band

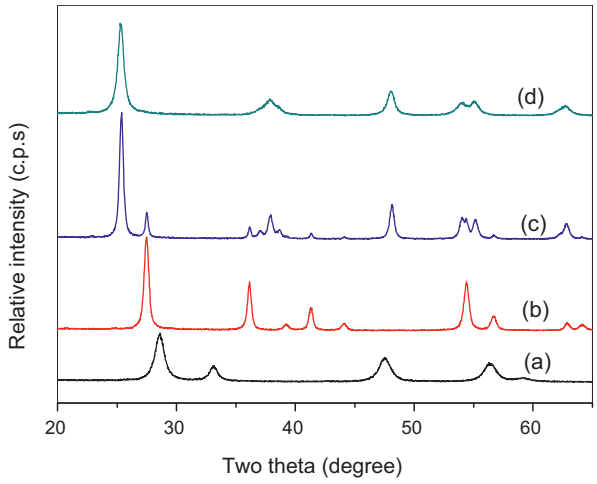

Fig. 1. XRD patterns of (a) CeO_2, (b) sRT, (c) P25, and (d) cAT. Note that CeO_2 and sRT were prepared at 400 °C..

gap energy of CeO_2/TiO_2, estimated by a derivative method [32], was also similar to that of parent TiO_2. These observations indicate that CeO_2/TiO_2 is a simple mixture of CeO_2 and TiO_2, and has similar physical parameters of TiO_2 as does the parent TiO_2.

3.2. Effect of CeO_2 loading

In this study, sRT and CeO_2 were separately obtained at 400 °C, and then they were mixed together at different ratios. Fig. 2A shows the time profiles of phenol degradation in aerated aqueous suspension. First of all, bare sRT and CeO_2 were active and nearly not active, respectively. The latter is probably due to the poor crystallinity of CeO_2 (Fig. S6A), which will be discussed below. Second, CeO_2/sRT was not only active, but also more active than bare sRT. Third, the time profile of phenol degradation satisfactorily fitted to the pseudo-first-order rate equation. As the weight percent of CeO_2 in the mixed oxide increased, the apparent rate constants of phenol degradation (k_{obs}) increased, and then decreased. A maximum value of k_{obs} for phenol degradation was observed with 1.5 wt% CeO_2/sRT, which was approximately 1.6 times that measured with bare sRT. Considering that these catalysts have different surface area (A_{sp}), the values of k_{obs} were then normalized with A_{sp}, and the result is shown in Fig. 2B. This specific rate of phenol degradation obtained with CeO_2/sRT was also larger than that measured with bare sRT. Since CeO_2 is nearly inactive and TiO_2 phase is similar in these samples (Table S1), it follows that CeO_2 has a positive effect on the photocatalytic activity of rutile TiO_2 for phenol degradation in aerated aqueous suspension.

3.3. Effect of sRT synthesis temperature

It has been reported that the intrinsic photocatalytic activity of TiO_2 increases with its synthesis temperature (T_s), regardless of the solid structures in the forms of anatase, rutile and their mixture [29,30]. Then it is necessary to examine the effect of T_s on the apparent activity of CeO_2/sRT. For this purpose, sRT was first prepared at 100–900 °C, and then mixed with 1.5 wt% of CeO_2 (which was prepared at 400 °C). Fig. 3 shows the result of phenol degradation measured in an aerated aqueous suspension. First of all, the apparent photocatalytic activity of sRT was a function of T_s, as reported early in the literature [2,29]. A maximum activity of sRT was observed at 300 °C, probably due to the combined effect of crystallinity and surface area (Table S2). Second, the apparent photocatalytic activity of CeO_2/sRT was not only a function of T_s, but also higher than that of bare sRT at given T_s. Interestingly, the k_{obs} ratio of CeO_2/sRT to sRT increased with the increase of T_s (Fig. 3B). This rate enhancement with T_s implies that the high intrinsic photocatalytic activity of rutile TiO_2 at high T_s can be explored through CeO_2 loading. As a result, phenol degradation over sRT become fast on the addition of CeO_2. This issue of CeO_2 effect will be further discussed below.

3.4. Effect of CeO_2 synthesis temperature

In this study, CeO_2 was prepared at T_s = 400–900 °C, and then sRT obtained at 400 °C was mixed with 1.5 wt% of CeO_2. Fig. 4A shows the result of phenol degradation in an aerated aqueous suspension, measured with CeO_2/sRT and parent CeO_2. In this case, bare CeO_2 became more active, as its T_s was increased. This result obtained from phenol degradation is similar to those observed from organic dye degradation [14,15], presumably ascribed to the increased crystallinity of CeO_2 (Table S3) that improves the efficiency of charge separation. However, the photocatalytic activity of CeO_2/TiO_2 decreased with the increase of T_s. This "unexpected" result is not due to the effect of surface area. After the value of k_{obs} for phenol degradation was normalized with the value of A_{sp} for CeO_2, the sample containing CeO_2 prepared at 400 °C is still more active than others (Fig. 4B). Since the TiO_2 phase is similar in these samples (Table S3), it follows that CeO_2 produced at low T_s is better

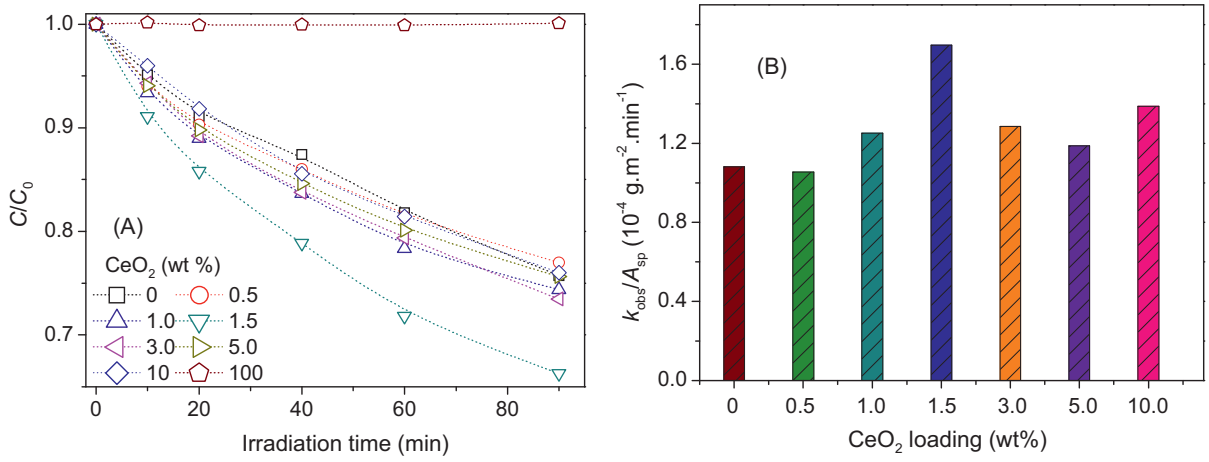

Fig. 2. Photocatalytic degradation of phenol over CeO_2/sRT in aerated aqueous suspensions. Both CeO_2 and sRT were prepared at 400 °C. The symbols k_{obs} and A_{sp} represent the apparent rate constant of phenol degradation and the BET surface area of the catalyst, respectively.

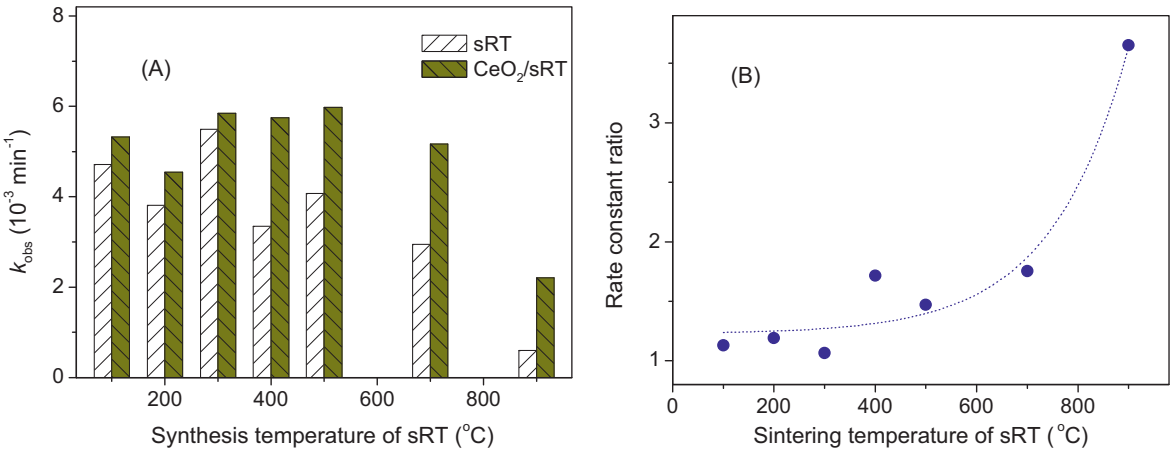

Fig. 3. (A) Apparent rate constants of phenol degradation in the aerated aqueous suspensions of sRT and 1.5 wt % CeO_2/sRT. (B) The rate constant ratio of CeO_2/sRT to sRT. Note that CeO_2 was prepared at 400 °C.

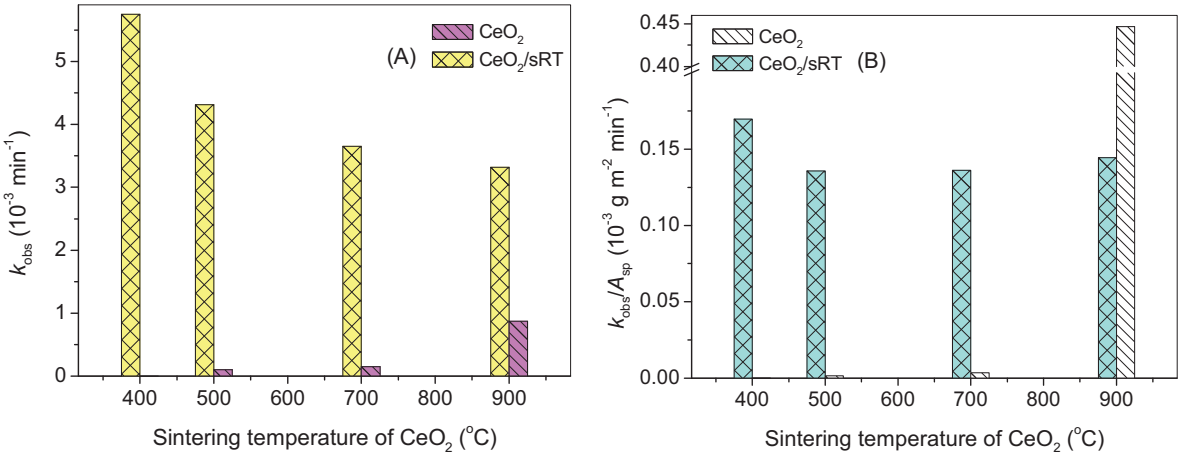

Fig. 4. (A) Apparent rate constants of phenol degradation in the aerated aqueous suspensions of CeO_2 and 1.5 wt% CeO_2/sRT. (B) The BET surface area normalized rate constants. sRT was obtained at 400 °C.

than that prepared at high T_s to improve the photocatalytic activity of TiO_2.

The color of bare CeO_2 changed with its synthesis temperature, from pale-yellow at 400 °C, to white at 900 °C (Fig. S8). This color change of CeO_2 with T_s has been intensively studied in the literature [14,15], ascribed to the changes of oxygen vacancies and Ce^{3+} ions in the bulk and on the surface of CeO_2. After the sample is thermally treated in air, these defects are removed, with the formation of a white and stoichiometric CeO_2 [11]. A study of DRS showed that as T_s increased, the absorption edge of CeO_2 was blue-shifted, from 450 nm at 400 °C, to 380 nm at 900 °C (Fig. 5). Through a derivative method [32], the band gap energy (E_g) of bare CeO_2 was estimated, which was 2.73, 2.79, 3.02 and 3.29 eV for the samples obtained at 400, 500, 700 and 900 °C, respectively. These values of E_g are smaller than, or close to that of bulk CeO_2 (3.2 eV) [15,35]. The narrowing in the band gap is due to the energy levels of oxygen vacancies and Ce^{3+} located in the band gap of CeO_2 [14]. Higher is the defect concentration, larger will be the reduction in the band gap. In other words, the defect concentration of CeO_2 decreases with T_s. A similar result was also obtained from XRD analysis. The lattice parameter of cubic CeO_2 in database is 0.5411 nm. The calculated lattice parameters for the CeO_2 samples obtained at 400, 500, 700 and 900 °C were 0.5413, 0.5406, 0.5406, and 0.5404 nm, respectively. Since the crystal size of CeO_2 increased with T_s (Table S3), the observed lattice expansion with reducing the crystal size is attributed to the oxygen vacancies and Ce^{3+} present on the oxide surface [35,36]. This change of defect concentration with T_s is in good agreement with that observed in the apparent photocatalytic activity of CeO_2/TiO_2 for phenol degradation in aerated aqueous suspension (Fig. 4A). Since these defects of CeO_2 can store and

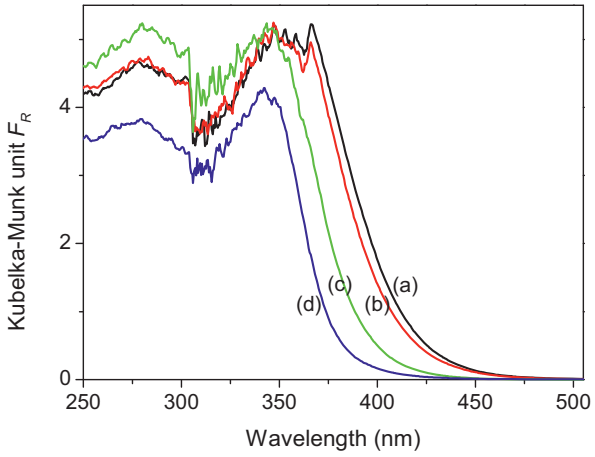

Fig. 5. DRS of CeO_2 prepared at the temperatures of (a) 400, (b) 500, (c) 700, and (d) 900 °C.

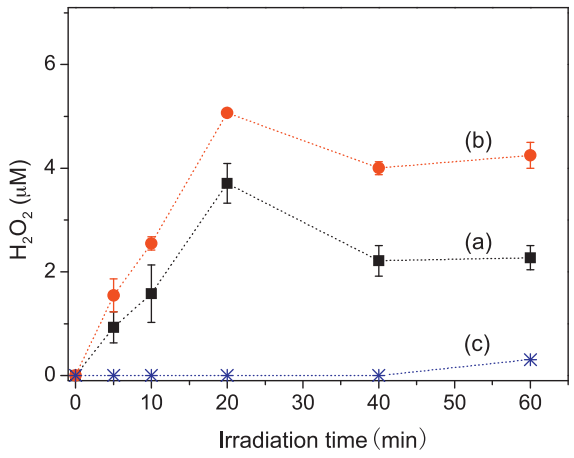

Fig. 6. Formation of H_2O_2 over (a) sRT, (b) 1.5 wt% CeO_2/sRT, and (c) CeO_2 in an aerated aqueous suspension containing 0.43 mM phenol. Note that sRT and CeO_2 were separately obtained at 400 °C.

release O_2 [10–13], it is highly possible that CeO_2 takes up O_2 from aqueous solution, and then transfers the adsorbed O_2 to rutile TiO_2 nearby. This would result into increase not only in the rate of O_2 reduction, but also in the efficiency of the charge separation of TiO_2 for phenol degradation.

To provide evidence for the enhanced reduction of O_2, the formation of H_2O_2 was examined by a colorimetric method. Experiment was carried out in the presence of phenol as a hole scavenger to speed up the reduction of O_2. Three catalysts were used, which were bare CeO_2 and sRT prepared at 400 °C, and their mixture (Fig. 6). Under UV light, not only H_2O_2 was detectable, but also its formation rate over 1.5 wt% CeO_2/sRT was notably larger than that over bare sRT. Under similar conditions, CeO_2 itself was nearly inactive. This trend in the activity for the production of H_2O_2 is in agreement with that for the photocatalytic degradation of phenol in aerated aqueous solution (Fig. 2). Note that after 20 min, H_2O_2 concentration decays with time, indicative of H_2O_2 consumption through other pathways, such as the direct photolysis of H_2O_2 to form •OH radicals.

3.5. *Effect of TiO_2 crystal structures*

In nature, TiO_2 exists in three crystal forms of anatase, rutile and brookite, among which brookite is difficultly synthesized. Then, a question arose regarding whether anatase after mixed with CeO_2 can result in the improved photocatalytic activity. With this concern, three TiO_2 samples of anatase (cAT), rutile (sRT at 400 °C), and P25 (a mixture of anatase and rutile), were used as starting materials. Then, each of them was mixed with 1.5 wt% of CeO_2 (obtained at 400 °C) by using similar procedures. Fig. 7A shows the results of phenol degradation measured in aerated aqueous suspension under UV light. First of all, the bare TiO_2 showed an increasing activity of P25 > cAT > sRT. Second, a similar trend was also observed with the CeO_2-mixed TiO_2. However, CeO_2 was positive only to sRT, while the activities of CeO_2/cAT and CeO_2/P25 were slightly lower than those of cAT and P25, respectively. These observations with anatase and P25 are not in agreement with those reported in the literature, probably due to the physical parameters of TiO_2 having changed after modification with CeO_2 [16–27]. In the present work, the TiO_2 phase in CeO_2/TiO_2 is nearly the same as parent TiO_2 (Table S4). In other words, the different effects of CeO_2 on the photocatalytic activities of anatase, rutile and P25 observed here are surely due to the effect of CeO_2.

The observed discrepancy of CeO_2 effect between anatase and rutile is probably due to the issue of O_2 adsorption on the oxide in water. In principle, e_{cb}^- and h_{vb}^+ are photogenerated in a pair. Then any delay in the consumption of e_{cb}^- by O_2 would retard further generation of the charge carriers, consequently making the photocatalyst deactivated. In a previous study [29,30], we have proposed that anatase has a stronger affinity to O_2 in water than rutile. Because of that, anatase usually shows a higher photocatalytic activity than rutile for organic degradation in aerated aqueous solution. As pointed out above, CeO_2 has ability to store and release O_2. It is conceivable that the amount of O_2 adsorbed on CeO_2 in aqueous solution is higher than that on sRT, but lower than those on cAT and P25. As a result, a positive effect of CeO_2 has been observed with sRT, not with cAT and P25 (Fig. 7A). This hypothesis of O_2 adsorption needs to be proved. However, no simple method is available to measure the amount of O_2 adsorbed on the metal oxide in water.

In order to evaluate the catalyst activity with the same amount of O_2 adsorbed on the catalyst surface, Ag^+ was used as alternative electron scavenger for phenol degradation under N_2 [29,30]. In this case, phenol degradation did not follow the apparent first-order kinetics anymore, because Ag^+ concentration decreased with time, due to its reduction to Ag (Fig. S10). Then, only the initial rate of phenol degradation (R_0) at the first 10 min was measured. Moreover, prior to light irradiation, the amount of Ag^+ adsorbed on the oxide (q_{Ag}) was determined. Since phenol degradation is the outcome of Ag(I) reduction, the value of R_0 was normalized with q_{Ag}, and the

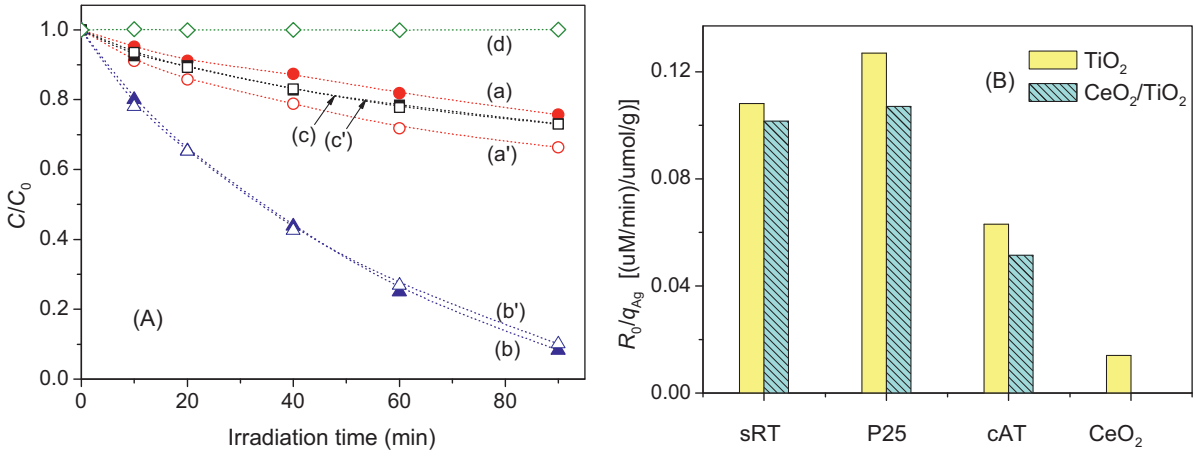

Fig. 7. (A) Phenol degradation in the aerated aqueous suspensions of (a) sRT, (b) P25, (c) cAT, and (d) CeO_2. Both sRT and CeO_2 were prepared at 400 °C. The curves (a′)–(c′) were the corresponding samples loaded with 1.5 wt% CeO_2. (B) The same experiments performed under N_2 in the presence of 1.0 mM $AgNO_3$ as electron scavenger. The symbols q_{Ag} and R_0 represent the initial amount of Ag^+ adsorbed, and the initial rate of phenol photodegraded, respectively.

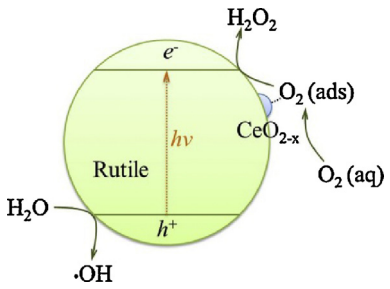

Scheme 1. Possible mechanism for the enhanced activity of CeO_2/TiO_2.

result is shown in Fig. 7B. Surprisingly, this specific rate of phenol degradation (R_0/q_{Ag}) obtained with CeO_2/TiO_2 was always smaller than that measured with TiO_2, whatever the TiO_2 component is sRT, cAT and P25. Such detrimental effect of CeO_2 on the intrinsic activity of TiO_2 is probably to the shielding effect of CeO_2 that reduces the number of photons reaching TiO_2. The absorption spectrum of CeO_2 largely overlaps with that of TiO_2 (Fig. 5). This observation give a further support of the above hypothesis that CeO_2 in CeO_2/TiO_2 plays a role of oxygen promoter for TiO_2 photocatalysis.

3.6. Possible mechanism

In the literature, the observed positive effect of CeO_2 on the photocatalytic activity of anatase TiO_2 is presumably ascribed to the interfacial charge transfer between CeO_2 and TiO_2 [16–27]. In order to verify the mechanism, the conduction band edge potentials (E_{CB}) for cAT, sRT, P25 and CeO_2 used in this work were all measured (Fig. S11 for details) [37,38]. Each oxide was coated onto an ITO electrode. Then the flat band potential (E_{fb}) for each film electrode in aqueous solution was determined through a Mott–Schottky plot. Finally, from the relationship between E_{fb} and E_{CB}, the value of E_{CB} was calculated. The estimated values of E_{CB} for the cAT, P25, sRT and CeO_2 electrodes in aqueous solution at pH 0 were −0.081, 0.010, 0.063, and 0.028 V *vs.* NHE (normal hydrogen electrode), respectively. According to these values of E_{CB}, the electron transfer from CeO_2 to sRT and the electron transfer from cAT or P25 to CeO_2 are all possible in thermodynamics. If these processes occur, the activity enhancement should be observed with each of the CeO_2-mixed TiO_2 samples. However, for phenol degradation under N_2 in the presence of $AgNO_3$, no activity enhancement was observed with any of the above CeO_2/TiO_2 (Fig. 7B). Therefore, the literature model of an interfacial charge transfer between TiO_2 and CeO_2 is not operative in the present study.

To interpret the observed higher activity of CeO_2/sRT than that of sRT, we propose that CeO_2 functions as O_2 supplier to TiO_2 photocatalysis (Scheme 1). Such oxygen transfer from CeO_2 to rutile TiO_2 would not only accelerate the reduction of O_2 to H_2O_2 (Fig. 6), but also facilitate the charge separation of rutile, further increasing the rates of surface reactions. As a result, the overall rate of phenol degradation on CeO_2/TiO_2 is notably increased, as compared to that occurring on bare TiO_2.

Furthermore, the value of E_{CB} for sRT is more positive than the standard redox potential for the $O_2/HO_2^{\bullet}$ couple (−0.05 V *vs.* NHE). Then the one-electron reduction of O_2 by e_{cb}^- on sRT is not allowed in thermodynamics. However, phenol degradation over sRT or CeO_2/sRT in aerated aqueous suspension well follows the first-order kinetics (Fig. 2A). Then, the observed reduction of O_2 to H_2O_2 on the irradiated catalyst would be ascribed to one two-electron transfer pathway. This multi-electron transfer of rutile, together with its weak affinity to O_2 in water, would be very slow for phenol degradation, as compared to the reactions occurring on anatase. However, sRT prepared at 400 °C shows an apparent activity not much lower than that of cAT (Fig. 7A), even though its BET surface area (31 m^2/g) is much lower than that of cAT (126 m^2/g). We speculate that the commercial product of cAT is produced at a temperature lower than 400 °C [30].

Since the CeO_2 sample produced at low temperature has a large positive effect on the photocatalytic activity of TiO_2 (Fig. 4), it follows that the oxygen vacancies and Ce^{3+} sites present on the surface of nonstoichiometric CeO_2 are the active sites for the uptake of O_2 from water. On the other hand, CeO_2 produced at a high temperature is well-crystallized, and therefore it shows a good photoactivity for phenol degradation. But this well-crystallized CeO_2 is lack of enough defects, and thus it exhibits a small or negative effect on the photocatalytic activity of TiO_2 (Fig. 4A).

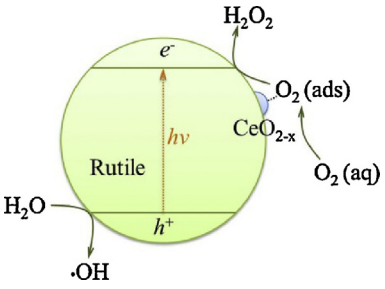

4. Conclusions

In this work, we have demonstrated that a simple mixing of rutile TiO_2 with 1.5 wt% of CeO_2 can increase the activity by 60% for phenol degradation in aerated aqueous suspension under UV light. Since the TiO_2 phase remains intact, the observed activity enhancement of rutile TiO_2 is surely due to a positive effect of CeO_2. Strikingly, a large activity enhancement of CeO_2/TiO_2 is observed with CeO_2 prepared at low temperature, and with rutile prepared at high temperature. By using Ag^+ as electron scavenger, and through measurement of H_2O_2 production, and estimation of conduction band potentials, we propose that CeO_2 can store and release O_2 to TiO_2 nearby, consequently exploring the masked photocatalytic activity of rutile for O_2 reduction and phenol degradation at the solid–liquid interface. Since the reduction of O_2 is the rate determining step in TiO_2 photocatalysis [1–3], the present work highlights the possibility that a CeO_2-based materials may find application as oxygen promoter of TiO_2 photocatalyst facilitating organic degradation in aqueous environment.

Competing interest

The authors declare no competing financial interest.

Appendix A. Supplementary data

Supplementary data associated with this article can be found, in the online version, at http://dx.doi.org/10.1016/j.apcatb.2014.11.029.

References

[1] M.R. Hoffmann, S.T. Martin, W. Choi, D.W. Bahnemann, Chem. Rev. 95 (1995) 69–96.
[2] C.L. Carp, A. Huisman, Reller, Prog. Solid State Chem. 32 (2004) 33–177.
[3] T. Tachikawa, M. Fujitsuka, T. Majima, J. Phys. Chem. C 111 (2007) 5259–5275.
[4] A.V. Emeline, X. Zhang, M. Jin, T. Murakami, A. Fujishima, J. Phys. Chem. B 110 (2006) 7409–7413.
[5] B. Ohtani, Y. Ogawa, S. Nishimoto, J. Phys. Chem. B 101 (1997) 3746–3752.
[6] M. Kong, Y. Li, X. Chen, T. Tian, P. Fang, F. Zheng, X. Zhao, J. Am. Chem. Soc. 133 (2011) 16414–16417.
[7] Z. Li, Y. Xu, J. Phys. Chem. C 117 (2013) 24360–24367.
[8] A.M. Peiro, C. Colombo, G. Doyle, J. Nelson, A. Mills, J.R. Durrant, J. Phys. Chem. B 110 (2006) 23255–23263.
[9] K. Lv, Y. Xu, J. Phys. Chem. B 110 (2006) 6204–6212.

[10] Y. Zhang, S. Andersson, S.S. Muhammed, Appl. Catal. B 6 (1995) 325–337.
[11] V.V. Pushkarev, V.I. Kovalchuk, J.L. d'Itri, J. Phys. Chem. B 108 (2004) 5341–5348.
[12] P. Dutta, S. Pal, M.S. Seehra, Y. Shi, E.M. Eyring, R.D. Ernst, Chem. Mater. 18 (2006) 5144–5146.
[13] L. Wu, M. Li, J. Howe, H.M. Meyer, S.H. Overbury, Langmuir 26 (2010) 16595–16606.
[14] B. Choudhury, P. Chetri, A. Choudhury, RSC Adv. 4 (2014) 4663–4671.
[15] A.B. Sifontes, M. Rosales, F.J. Méndez, O. Oviedo, T. Zltan, J. Nanomater. (2013) 265797.
[16] M.J. Muñoz-Batista, M.N. Gómez-Cerezo, A. Kubacka, D. Tudela, M. Fernández-Garcia, ACS Catal. 4 (2014) 63–72.
[17] S. Ghasemi, S. Rahman Setayesh, A. Habibi-Yangjeh, M.R. Hormozi-Nezhad, M.R. Gholami, J. Hazard. Mater. 199–200 (2012) 170–178.
[18] T. Tong, J. Zhang, B. Tian, F. Chen, D. He, M. Anpo, J. Colloid Interface Sci. 315 (2007) 382–388.
[19] W. Xue, G. Zhang, X. Xu, X. Yang, C. Liu, Chem. Eng. J. 167 (2011) 397–402.
[20] Y. Zhang, A.H. Yuwono, J. Wang, J. Li, J. Phys. Chem. C 113 (2009) 21406–21412.
[21] F. Galindo, R. Gomez, M. Aguilar, J. Mol. Catal. A 282 (2008) 119–125.
[22] J. Xiao, T. Peng, R. Li, Z. Peng, C. Yan, J. Solid State Chem. 179 (2006) 1161–1170.
[23] G. Li, C. Liu, Y. Liu, Appl. Surf. Sci. 253 (2006) 2481–2486.
[24] N. Aman, P.K. Satapathy, T. Mishra, M. Mahato, N.N. Das, Mater. Res. Bull. 47 (2012) 179–183.
[25] M. Sidheswaran, L.L. Tavlarides, Ind. Eng. Chem. Res. 48 (2009) 10292–10306.
[26] B. Choudhury, B. Borah, A. Choudhury, Photochem. Photobiol. 88 (2012) 257–264.
[27] G. Li, D. Zhang, J.C. Yu, Phys. Chem. Chem. Phys. 11 (2009) 3775–3782.
[28] Y. Zhang, H. Xu, Y. Xu, H. Zhang, Y. Wang, J. Photochem. Photobiol. A 170 (2005) 279–285.
[29] Q. Sun, Y. Xu, J. Phys. Chem. C 114 (2010) 18911–18918.
[30] S. Cong, Y. Xu, J. Phys. Chem. C 115 (2011) 2116–21168.
[31] M. Anpo, T. Shima, S. Kodama, Y. Kubokawa, J. Phys. Chem. 91 (1987) 4305–4310.
[32] D. Chakrabarti, S. Ganguli, Chaudhuri, Physica E 24 (2004) 333–342.
[33] G.C.B. Cave, D.N. Hume, Anal. Chem. 24 (1952) 1503–1505.
[34] H. Bader, V. Sturzenegger, J. Hoigné, Water Res. 22 (1988) 1109–1115.
[35] F. Zhang, S.W. Chan, J.E. Spanier, E. Apak, Q. Jin, R.D. Robinson, I.P. Herman, Appl. Phys. Lett. 80 (2002) 127–129.
[36] S. Deshpande, S. Patil, S. Kuchibhatla, S. Seal, Appl. Phys. Lett. 87 (2005) 133113.
[37] S.N. Frank, A.J. Bard, J. Am. Chem. Soc. 97 (1975) 7427–7433.
[38] X.F. Cheng, W.H. Leng, D.P. Liu, Y.M. Xu, J. Phys. Chem. C 112 (2008) 8725–8734.